

Classical Nuclear Motion in Quantum Transport

Claudio Verdozzi,* Gianluca Stefanucci, and Carl-Olof Almbladh
Solid State Theory, Lund University, Sölvegatan 14 A, 223 62 Lund, Sweden
(Dated: February 8, 2020)

An *ab initio* quantum-classical mixed scheme for the time evolution of electrode-device-electrode systems is introduced to study nuclear dynamics in quantum transport. Two model systems are discussed to illustrate the method. Our results provide the first example of current-induced molecular desorption as obtained from a full time-dependent approach, and suggest the use of AC biases as a way to tailor electromigration.

PACS numbers: 72.10.Bg, 73.63.-b, 63.20.Ry, 63.20.Kr

The problem of electron-nuclei interaction (ENI) in solids has a long and important history, which goes back to the early days of quantum mechanics. Since then, the ENI has become one of the pillar concepts of our understanding in condensed matter [1]. Also, the increase in computer power and the introduction of *ab-initio* molecular dynamics methods [2] have made possible a quantitative understanding of the ENI in many materials.

Recent advances in nanotechnology, however, pose new questions about the ENI in out-of-equilibrium open systems at the nanoscale [3]. Among the techniques used to study the ENI in this context, quantum transport experiments stand out as a special case, since charge conduction is at the same time a way to characterize the nanodevice and a property to be exploited in its operating regime. A case in point is that of molecular junctions, where electron injection can stimulate local vibrations [4, 5] and possibly electromigration [6]. Assessing and engineering the nature of ENI is then a key ingredient to increase the device efficiency [7, 8]. To date, most theoretical studies have addressed the ENI in steady-state phenomena [9, 10, 11, 12, 13, 14, 15] and often only perturbatively in the nuclear displacements [13, 14, 15]. Going beyond the harmonic approximation and including the ENI in a first-principles time-dependent framework is a difficult theoretical task which has received so far scarce attention [16, 17].

In this work we propose an approach to time-dependent quantum transport which treats electronic and classical nuclear motion on equal footing. Following Refs. [18, 19, 20], in the initial ground state the device is in contact to seminfinite left and right leads. We illustrate the method with two spinless model devices, where the electrons interact only via the ENI: a Holstein wire (D1), and a diatomic molecule (D2) where full nuclear dynamics is allowed. Our results show that: i) For weak electron-phonon (EP) couplings, D1 exhibits an almost periodic nuclear displacement (with period=1/density), reminiscent of a Peierls distortion. On applying a DC bias, the nuclei oscillate (with decreasing amplitude) and the period changes to accommodate the current flow. ii) On increasing the EP coupling, D1 changes from conducting to insulating. iii) D2 is deformed by a small,

suddenly switched on DC bias. Above a critical value of the bias, the molecule dissociates. This is the single most important result of this work. To our knowledge, it provides the first example of current-induced molecular desorption as emerging from the exact evolution dynamics of a nanodevice. iv) The desorption can be tuned by the intensity and frequency of an AC bias, suggesting a way to control electromigration in molecular devices.

We consider a central region C coupled to a left (L) and a right (R) electrode, where the nuclei are clamped. In C, electrons interact with a classical field $\mathbf{x} = (x_1, \dots, x_N)$ that accounts for the nuclear dynamics. The Hamiltonian for region C reads

$$\hat{H}_C[\mathbf{x}] = \sum_{ij=1}^M V_{ij}(\mathbf{x}) c_i^\dagger c_j, \quad (1)$$

where M is the number of one-electron states of C. In the one-particle scheme of time-dependent density functional theory [21], V_{ij} would be the (i, j) matrix element of the Kohn-Sham Hamiltonian. The nuclear dynamics is described by $H_{\text{cl}} = \sum_{k=1}^N p_k^2/(2m_k) + U_{\text{cl}}(\mathbf{x})$ where p_k is canonically conjugated to x_k and $U_{\text{cl}}(\mathbf{x})$ is the classical potential. The time evolution of the system is governed by the following equations

$$i \frac{d}{dt} |\Psi\rangle = \hat{H}_{\text{el}} |\Psi\rangle, \quad (2)$$

$$m_k \frac{d^2 x_k}{dt^2} = -\frac{\partial}{\partial x_k} \left(U_{\text{cl}} + \langle \Psi | \hat{H}_C | \Psi \rangle \right), \quad (3)$$

where $|\Psi(t)\rangle$ is the many-electron state at time t , and $\hat{H}_{\text{el}}[\mathbf{x}]$ is the electron Hamiltonian of the contacted system L+C+R. Given a configuration \mathbf{x} , $\hat{H}_{\text{el}}[\mathbf{x}]$ is a free-particle Hamiltonian. The many-electron ground state $|\Psi_g[\mathbf{x}]\rangle$ consists of bound, resonant, fully reflected waves, and left (and right) going scattering states. The parametric dependence of \hat{H}_{el} on \mathbf{x} renders every eigenstate a function of \mathbf{x} . The value of the coordinates $\mathbf{x} = \mathbf{x}_g$ in the ground state can be computed using a damped ground-state dynamics. Starting from an initial \mathbf{x}_0 the coordinates are evolved according to $m_k \ddot{x}_k = -\gamma \dot{x}_k - \partial \left(U_{\text{cl}} + \langle \Psi_g | \hat{H}_C | \Psi_g \rangle \right) / \partial x_k$, with γ the friction

coefficient. Due to the multivalley nature of the potential, the damped dynamics might not converge to \mathbf{x}_g . To rule out this possibility, we have found the energy minimum of system C contacted to two finite electrodes of length L , determined $\mathbf{x}_g(L)$, and used its extrapolated value $\mathbf{x}_g(L \rightarrow \infty)$ as initial condition \mathbf{x}_0 .

Having the ground state \mathbf{x}_g and the corresponding set $\{\psi\}$ of one-electron orbitals, we apply an external bias and evolve the system. Assuming metallic electrodes and instantaneous screening, the size of C is chosen so that the potential drop at any time occurs entirely in C. Thus, the time-dependent part of the Hamiltonian \hat{H}_η , $\eta = \text{L,R}$, describing the left and right electrode is a spacially uniform shift $U_\eta(t)$. We use a novel mixed quantum-classical evolution algorithm, which combines a recently proposed generalization of the Crank-Nicholson method [20] for the $\{\psi\}$ with a Verlet-like integrator for the \mathbf{x} . Schematically, in terms of the discretized time $t_m = 2m\delta$,

$$\left\{ \begin{array}{l} \{\psi^{(m+1)}\} = \{S[t_m, \mathbf{x}^{(m)}]\psi^{(m)}\} \\ \\ \left\{ \begin{array}{l} p_k^{(m+1)} = p_k^{(m)} + 2\delta F_k[\mathbf{x}^{(m)}, \{\psi^{(m+1)}\}] \\ x_k^{(m+2)} = x_k^{(m)} + 4\delta p_k^{(m+1)}/m_k \\ p_k^{(m+2)} = p_k^{(m+1)} + 2\delta F_k[\mathbf{x}^{(m+2)}, \{\psi^{(m+1)}\}] \end{array} \right. \\ \\ \{\psi^{(m+2)}\} = \{S[t_{m+1}, \mathbf{x}^{(m)}]\psi^{(m+1)}\} \end{array} \right. \quad (4)$$

with $\psi^{(m)} = \psi(t_m)$, $\mathbf{x}^{(m)} = \mathbf{x}(t_m)$ and $\mathbf{p}^{(m)} = \mathbf{p}(t_m)$. The unitary matrix S depends on time through $\mathbf{x}(t)$ and the time-dependent bias $U_\eta(t)$, $\eta = \text{L,R}$. Full details of the electronic evolution can be found in Ref. [20]. The force $F[\mathbf{x}, \{\psi\}]$ is given by the r.h.s. of Eq.(3).

To illustrate the method, we describe electrodes L and R in terms of one-dimensional tight-binding Hamiltonians with a hopping V between nearest neighbour sites. Left and right going scattering states have energy ε within the band $(-2|V|, 2|V|)$ and can be obtained by solving the Schrödinger equation in C with appropriate boundary conditions. Bound state eigenenergies $\varepsilon_b < -2|V|$ satisfy $\text{Det}[\varepsilon_b \mathbf{1} - \mathbf{H}_C - \Sigma(\varepsilon_b)] = 0$, and the associated wavefunction is given in C by the kernel of $[\varepsilon_b \mathbf{1} - \mathbf{H}_C - \Sigma(\varepsilon_b)]$ (\mathbf{H}_C is the projection of \hat{H}_C onto the one-electron Hilbert space, $\Sigma(\omega)$ is the embedding self-energy). The non-trivial topology of region C might also lead to states rigorously confined in C (see below). These are resonant eigenstates of the uncontacted \mathbf{H}_C with zero amplitude at the interface with the two electrodes.

Model device D1. The semiclassical Holstein model is a valuable tool to gain insight into many aspects of the EP interaction [22, 23]. Here, we investigate time-dependent transport through a Holstein wire described by

$$\hat{H}_C = V \sum_{i=-M}^{M-1} (c_i^\dagger c_{i+1} + \text{h.c.}) - g \sum_{i=-M}^M x_i \hat{n}_i, \quad (5)$$

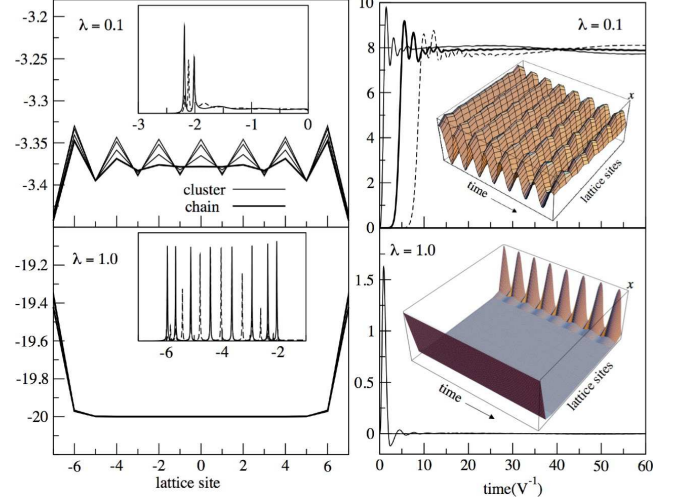


FIG. 1: Left panel: Ground state displacement x_i , $i = -7, \dots, 7$, at weak ($\lambda = 0.1$) and strong ($\lambda = 1.0$) coupling. Thin lines correspond to the $\mathbf{x}(L)$ of a ring with $L = 200, 400$ and 500 . The thick line is the converged \mathbf{x}_g . The inset shows the LDOS (energy in units of $|V|$) on site -6 (dashed line) and site 0 (solid line). Right panel: $I_{\text{L,R}}(t)$ (in units of $10^{-2}|V|$) at weak and strong coupling along the bond $(-7, -6)$ (solid thin), $(0, 1)$ (solid thick) and $(6, 7)$ (dashed) after the sudden switching on of a bias $U_{\text{L}} = 0.5|V|$ in electrode L. The insets show a 3D plot of $\mathbf{x}(t)$ between $t = 0$ and $t = 480|V|^{-1}$ (in the top panel the range of \mathbf{x} is between -3.2 and -4 while in the bottom panel is between -19.4 and -20).

where $\hat{n}_i = c_i^\dagger c_i$ is the local density operator and x_i are the phonon coordinates. The latter move in the classical potential $U_{\text{cl}}(\mathbf{x}) = \frac{1}{2} \sum_{i=-M}^M m_i \omega_0^2 x_i^2$. The strength of the EP interaction is determined by the dimensionless parameter $\lambda = g^2/(2V\omega_0)$. We consider D1 at half-filling ($\varepsilon_F = 0$) in the adiabatic regime ($\alpha = \omega_0/V = 0.1$) and specialize to the weak ($\lambda = 0.1$) and strong ($\lambda = 1$) coupling cases. In Fig. 1, left, we plot the displacement of the ground-state coordinates for a region C ($M = 7$) embedded in a ring of length $L = 200, 400, 500$ (the choice of a ring stems from the appealing feature of having twice degenerate delocalized states, as the infinite system). The value \mathbf{x}_g for the infinite system is obtained by a damped ground-state dynamics, as described above. We have discretized the energy spectrum between $-2|V|$ and ε_F by taking $N_k = 500$ wave functions distributed according to the density of states. We also checked the convergence of \mathbf{x}_g against a larger N_k . For $\lambda = 0.1$, a tendency towards a Peierls distortion is clearly seen. The finite size of C prevents an exact periodicity P in x_i . Though, an even-odd behavior as a function of i is still manifest, in agreement with the general result $P = 1/n$ (in our case, the average density $n = 0.5$). The inset shows the local density of states (LDOS) in two points of C, the first close to the interface and the second in the center. At $\varepsilon < -2|V|$ we observe three peaks due to three bound states. The picture changes dramatically at

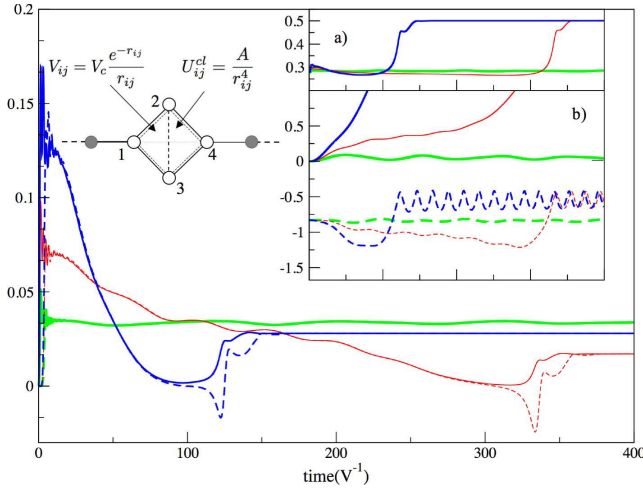


FIG. 2: $I_{L,R}(t)$ (in units of $|V|$) at the left (solid line) and right (dashed line) interface for $U_L = 0.25|V|$ (green [light grey]), $0.5|V|$ (red [thin dark grey]) and $1.0|V|$ (blue [thick black]). Inset a): Time dependent density n_3 of nucleus 3 (by symmetry $n_2 = n_3$ at any time). Inset b): $x_3(t)$ (solid line) and $y_3(t)$ (dashed line) of nucleus 3 (by symmetry $x_2 = x_3$ and $y_2 = -y_3$ at any time). Time scale and color coding in insets a) and b) is the same as in the main figure. A schematic of the device D2 embedded in the semi-infinite leads is also shown.

$\lambda = 1$: The number of bound states equals the dimension of C and, almost uniformly, $x_i \simeq -20$. Only the x_i close to the interfaces are slightly above this value.

In Fig. 1, right, we plot the time-dependent current in three different points of C after the sudden switching on of a bias $U_L = 0.5|V|$ in the left electrode. All calculations were performed with a time step $\delta = 0.01|V|^{-1}$. Both at weak and strong coupling the transient current is similar to the one obtained with clamped coordinates (not shown here), since the electron dynamics is much faster than the classical one. However, at $\lambda = 0.1$ we observe a steady current with superimposed oscillations of frequency ω_0 . This is not the case for $\lambda = 1$ due to the charge stiffness in C. All the $2M + 1 = 15$ bound states are occupied and no current fluctuations occur in the center and at the right interface (the inclusion of the Hartree potential would have led to a significant reduction of this excess density in C). A very short transient is observed at the left interface where region C is contacted with the biased electrode. The insets display the time-dependent Peierls distortion up to $t = 480|V|^{-1}$. For $\lambda = 0.1$ all the x 's oscillate with an amplitude that decreases exponentially (within our simulation time). The shape of the overall displacement changes in order to accomodate the net electron flow. The opposite happens for $\lambda = 1$ where no current flows and only the coordinates close to the left interface oscillate. We also considered the sudden removal of a bound electron, as obtainable for example by optical means: the results, not presented here, show that

D1 provides a strong transient oscillating response. On speculative grounds, this in turn suggests the possibility of using such behavior for ENI based photosensors.

Model device D2. We consider a central region C with the simplest non-trivial topology, a four-atom ring. This is our model molecular device D2, with nuclear positions $\mathbf{r}_i \equiv (x_i, y_i)$, $i = 1, \dots, 4$ (Fig. 2, top-left). In D2, only nuclei 2 and 3 are let to move in the xy plane. The origin of the xy plane is the midpoint of 1 and 4. For the hopping parameter we choose the form [24] $V_{i \neq j} = V_c \frac{e^{-r_{ij}}}{r_{ij}}$, $V_{i=j}=0$, where $r_{ij} = |\mathbf{r}_i - \mathbf{r}_j|$. The purely repulsive classical term is given by $U_{\text{cl}} = \frac{1}{2} \sum_{i \neq j} A / r_{ij}^4$. We tune the parameters V_c , A and r_{14} to ensure a reasonable domain of structural stability for D2. Choosing $V_c = 4V$, $A = 0.75|V|$ and $r_{14} = 2$, D2 is stable against deformations up to $\sim 10\%$ of the equilibrium distances. Also, we get the ground state positions $\mathbf{r}_2 = (0, 0.8313)$ and $\mathbf{r}_3 = -\mathbf{r}_2$ (the 2–3 symmetry remains true in the presence of the bias). The LDOS has two peaks below $-2|V|$ and hence two bound states. There is also a resonant state $|\psi\rangle = \frac{1}{\sqrt{2}}(|2\rangle - |3\rangle)$ with energy $|V_{23}| > 0$ inside the band. We study the system at half filling, under the influence of an external bias $U_L = 0.25, 0.5, 1.0$ (in units of $|V|$) which is switched on at $t = 0$. As for D1, $\delta = 0.01|V|^{-1}$, $N_k = 500$; for the masses of the nuclei 2 and 3 we choose $100|V|^{-1}$.

In Fig. 2 we plot the time dependent currents I_L and I_R at the left and right interfaces, respectively. At small bias $U_L = 0.25|V|$, the current rapidly increases and after a short transient (during which the nuclei remain essentially still) it starts to oscillate around a steady value. In the inset b) we show the corresponding nuclear dynamics. We observe that the equilibrium rhombic geometry changes and the molecule gets deformed in the biased system (nuclei 2 and 3 have damped oscillations around two new positions). We also notice from inset a) that the charge density of nuclei 2 and 3 slightly increases.

Highly interesting is the strong bias case $U_L = 1.0|V|$. The transient behavior is qualitatively similar to that of $U_L = 0.25|V|$, provided it is scaled down by a factor of ~ 3 . Later on, $I_{L,R}$ sharply decrease (rather than oscillating around a steady value) and become zero at $t_0 \simeq 100|V|^{-1}$. After t_0 , $I_{L,R}$ separate: I_L increases while I_R decreases, reaches a negative minimum and then increases to eventually re-join I_L at $t_1 \sim 160|V|^{-1}$. For $t > t_1$, $I_L \simeq I_R$ and their value equal the steady current (calculated from the Landauer formula) of the chain without nuclei 2 and 3. The behavior of $I_{L,R}$ can be understood looking at the nuclear dynamics (inset b): the force exerted by the electron flow is strong enough for atomic migration to occur. The nuclei 2 and 3 are pushed to the right by the current, overcome the confining potential and get dissociated from region C. Thereafter, they form a diatomic molecule vibrating along y (see inset b) and traveling along x at uniform speed. The pronounced

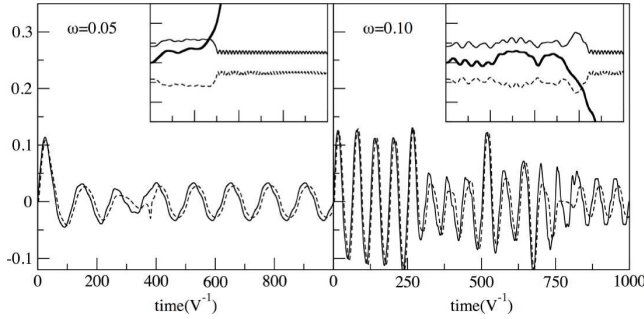


FIG. 3: Left panel: $I_{L,R}(t)$ (in units of $|V|$) at the left (solid line) and right (dashed line) interface for $U_L = 1.0|V|$, $\omega = 0.05|V|$. In the inset, $x_2(t) = x_3(t)$ (thick solid) and $y_2(t)$ (thin solid), $y_3(t)$ (dashed). The time scale is the same as in the main panel. Right panel: same as left, but with $\omega = 0.10|V|$. Left and right insets have the same vertical scale .

minimum of I_R shortly after t_0 is due to a sudden charge transfer from electrode R (via atom 4) to the diatomic molecule when nuclei 2 and 3 pass above 4. This is confirmed in inset a) where the charge density suddenly increases in correspondence of the minimum in I_R . We also note that the total density of the dissociated molecule is about 1 (exact charge quantization would have occurred in the adiabatic approximation only). In this case, the inclusion of the Hartree potential would not lead to any qualitative changes of the dissociation process. A more realistic model should also include the possibility for the molecule to get chemisorbed onto the electrode, to fragment etc., but this is beyond the scopes of the present work. At $U_L = 0.5|V|$, a delayed, but qualitatively similar dissociation is observed.

We next examined the response of D2 when subject to a high amplitude AC bias $U_L(t) = U_L \sin(\omega t)$, with $U_L = 1.0|V|$. At low ω (Fig. 3, left), the system qualitatively behaves as in the DC case, as clear from both current (main left) and coordinates (inset left) panels. The nuclei overtake the barrier before the change in $U_L(t)$ produces a force able to “recall” them back. Also, because of the slow rise of $U_L(t)$, the transient due to a suddenly switched on bias is not the primary cause for dissociation. After the desorption, $I_{L,R}$ oscillate as they would for a linear chain without nuclei 2 and 3. At larger ω (Fig. 3, right) the dissociation is delayed, since atoms 2 and 3 are recalled back a few times before leaving region C. Eventually, for high enough frequency ($> 0.3|V|$, not shown) atoms 2 and 3 oscillate without leaving C (within our simulation time). These model results point to a possible use of AC biases as a way to tailor molecular desorption in nanodevices.

In conclusion, we presented a mixed quantum-classical scheme to describe electron-nuclei interactions in quantum transport. The scheme is straightforwardly

amenable to an *ab-initio* implementation. Our model calculations show the necessity of a full time-dependent, full nuclear-dynamics approach to study non-equilibrium phenomena like, for example, current-induced dissociation. More generally, the results suggest that tailoring the electron-nuclear interaction at the nanoscale holds promise of future improvement in device performance.

We acknowledge useful discussions with G. J. Ackland, P. Bokes and E. N. Economou. This work was supported by the European Community 6th framework Network of Excellence NANOQUANTA (NMP4-CT-2004-500198).

* Electronic address: cv@teorfys.lu.se

- [1] J. M. Ziman, *Electron and Phonons*, Oxford U. P. (1960).
- [2] R. Car, and M. Parrinello, Phys. Rev. Lett. **55**, 2471 (1985).
- [3] *Electron-Phonon Interactions in Low-Dimensional Structures*, L. Challis ed., Oxford U. P., Oxford (2003).
- [4] M. A. Reed, C. Zhou, C. J. Muller, T. P. Burgin, and J. M. Tour, Science **278**, 252 (1997).
- [5] H. Park , J. Park, A. K. L. Lim, E. H. Anderson, A. P. Alivisatos and P. L. McEuen, Nature **407**, 57 (2000).
- [6] H. Yasuda and A. Sakai, Phys. Rev. B **56**, 1069 (1997).
- [7] P. Hyldgaard, Low Temp. Phys. **27**, 585 (2001).
- [8] A. A. Balandin, J. Nanosci. Nanotechnol. **5**, 1015 (2005).
- [9] E. G. Emberly and G. Kirczenow, Phys. Rev. B **64**, 125318 (2001).
- [10] T. N. Todorov, J. Hoekstra, and A. P. Sutton, Phys. Rev. Lett. **86**, 3606 (2001).
- [11] M. Brandbyge, K. Stokbro, J. Taylor, J. L. Mozos, and P. Ordejon, Phys. Rev. B **67**, 193104 (2003).
- [12] M. Di Ventra, S. T. Pantelis and N. D. Lang, Phys. Rev. Lett. **88**, 046801 (2002).
- [13] M. Paulsson, T. Frederiksen, and M. Brandbyge, Phys. Rev. B **72**, 201101(R), 2005.
- [14] T. Frederiksen, M. Brandbyge, N. Lorente and A.-P. Jauho, Phys. Rev. Lett. **93**, 256601 (2004).
- [15] K. Burke, R. Car and R. Gebauer, Phys. Rev. Lett. **94**, 146803 (2005).
- [16] Z. G. Yu, D. L. Smith, A. Saxena and A. R. Bishop, Phys. Rev. B **59**, 16001 (1999).
- [17] R. Lu and Z. R. Liu, J. Phys. Condens. Matter **17**, 5859 (2005).
- [18] M. Cini, Phys. Rev. B **22**, 5887 (1980).
- [19] G. Stefanucci and C.-O. Almbladh, Phys. Rev. B **69**, 195318 (2004).
- [20] S. Kurth, G. Stefanucci, C.-O. Almbladh, A. Rubio and E. K. U. Gross, Phys. Rev. B **72**, 035308 (2005).
- [21] E. Runge and E. K. U. Gross, Phys. Rev. Lett. **52**, 997 (1984).
- [22] S. Kumar and P. Majumdar, Phys. Rev. Lett. **94**, 136601 (2005).
- [23] G. Kopidakis, C. M. Sokoulis and E. N. Economou, Phys. Rev. B **51**, 15038 (1995).
- [24] L. Goodwin, A. J. Skinner and D. G. Pettifor, Europhys. Lett. **9**, 701 (1989).